Environmental Science
Water Research & Technology

Assessing Disinfection Byproduct Risks for Algal Impacted Surface Waters and the Effects of Peracetic Acid Pre-Oxidation

Journal:	*Environmental Science: Water Research & Technology*
Manuscript ID	EW-ART-03-2020-000237.R1
Article Type:	Paper

Assessing Disinfection Byproduct Risks for Algal Impacted Surface Waters and the Effects of Peracetic Acid Pre-Oxidation

Zachary T. Kralles[†], Kaoru Ikuma[‡], and Ning Dai[*†]

[†] Department of Civil, Structural and Environmental Engineering
University at Buffalo, the State University of New York, Buffalo, NY, 14260

[‡] Department of Civil, Construction and Environmental Engineering
Iowa State University, Ames, IA, 50011

[*]Corresponding author: Post address: 231 Jarvis Hall, Buffalo, NY 14260
Phone : (716) 645-4015 ; Fax : (716) 645-3667
Email : ningdai@buffalo.edu

Abstract

This study assessed the disinfection byproduct (DBP) risks of algal impacted surface waters and the effects of peracetic acid (PAA) pre-oxidation on DBP risks. Authentic samples from three eutrophic lakes were collected over a 13-week period during the algal bloom season. The formation of 11 DBPs (four trihalomethanes, four haloacetonitriles, two haloketones, and trichloronitromethane) in these samples were assessed under uniform formation conditions (UFC) approximating drinking water disinfection. Trihalomethanes formed in the greatest abundance (90–370 μg/L), followed by haloacetonitriles (6.5–87 μg/L), haloketones (0.4–11.4 μg/L), and trichloronitromethane (0.3–9.7 μg/L). Total chlorophyll, a common indicator of algal activity, was not found to correlate with DBP yields. On the other hand, the yields of trichloronitromethane and haloacetonitriles correlated with nitrite/nitrate concentrations and DON concentrations in the samples, respectively. PAA pre-oxidation reduced the formation of trihalomethanes in the subsequent UFC tests in 80% the samples, but promoted the formation of haloacetonitriles and trichloronitromethane in 70% and 50% of the samples, respectively. Analyses of DOC, DON, SUVA, and fluorescence excitation-emission matrices suggest that PAA pre-oxidation can alter the DBP precursors of a sample through the release of high haloacetonitrile/trichloronitromethane-yielding organic matter from algal cells and the oxidative transformation of existing and newly released dissolved organic matter. The results of this study, obtained from authentic surface water samples, suggest that mixed organic matter dynamics is an important consideration for the DBP risks of algal-impacted waters.

Water Impact Statement

Algae is more frequently impacting source waters due to climate change and eutrophication. Understanding its impacts on the formation of disinfection byproducts is crucial for water utilities to provide safe drinking water to the public. Peracetic acid, an emerging algal control method, may increase the cytotoxicity of the finished water by altering the profile of disinfection byproducts.

1. Introduction

Occurrence of algal blooms are becoming more frequent due to the warming climate and increasing nutrient input to surface waters.[1-3] Algal blooms impact drinking water quality by producing algal toxins, generating undesirable taste and odor, and increasing the level of dissolved organic matter.[4-6] Compared with natural organic matter (NOM) derived from plant debris, algal organic matter (AOM) is overall more hydrophilic, rendering it more difficult to be removed by conventional water treatment processes.[7-10] Additionally, AOM is rich in nitrogenous organic compounds such as proteins, amino sugars, and free amino acids that can serve as precursors of nitrogenous disinfection byproducts (N-DBPs).[11-14] Many N-DBPs exhibit 10-100 times higher toxicity than the regulated DBPs trihalomethanes (THMs) and haloacetic acids (HAAs).[15, 16]

Previous studies have shown that disinfection of AOM from laboratory algae cultures can lead to DBP formation. Fang et al. were among the first to conduct systemic investigation into the potential of AOM to form carbonaceous and nitrogenous DBPs. Using a suspension of cultured *Microcystis aeruginosa*, they showed that AOM had three times higher yield in two N-DBPs (trichloronitromethane (TCNM) and dichloroacetonitrile (DCAN)) than Suwannee River NOM.[11] Later studies showed that intracellular organic matter (IOM) has higher formation potential of THMs, haloacetonitriles (HANs), and haloketones (HKs) than extracellular organic matter (EOM).[12, 17-21] The DBP yields of AOM are also influence by the species of algae and their growth phase.[8, 11, 18] Chlorination of six algal species showed that *Microcystis aeruginosa*, the most common harmful bloom species,[22] had the highest DCAN formation potential.[8] In batch cultures of *Microcystis aeruginosa*, cells at the logarithmic phase exhibited the greatest yields of DCAN, TCNM, and haloketones (HKs), whereas cells at the lag phase exhibited the greatest yield of chloroform.[18]

While these laboratory studies using pure algae cultures unequivocally demonstrated that AOM is a source of DBP precursors, it is challenging to translate the findings directly to algal impacted surface waters: laboratory cultures do not replicate the natural variation in algal activity or the water quality of algal impacted waters. First, surface waters contain a mixture of allochthonous (i.e., terrestrially-derived) and autochthonous organic matter (e.g., AOM). Typical Suwannee River NOM contains mostly humic substances, whereas AOM released from *Microcystic aeruginosa* is as high as 53% in biopolymers.[23] Furthermore, there is evidence suggesting that model algae biopolymer compounds can abiotically interact with humic substances[24, 25] and Suwannee River NOM.[23] Field samples containing a mixture of organic matters can capture these dynamic processes and therefore may yield different observations from those derived from laboratory algae cultures. Second, algae in natural environments exhibit less distinct growth phases than those observed in laboratory cultures[26] and feature a much more diverse population.[27] Finally, DBP yields from algae cultures may be confounded by the presence of interfering species in the culture media. For example, nitrite, an algal metabolite present at high concentrations when nitrogen-fortified media (e.g., BG 11) is used[12] can promote the formation of TCNM during chlorination.[28, 29]

To date, only a limited number of studies investigated the DBP risk of algal impacted surface waters, with little attention given to N-DBPs. The formation potential of regulated THMs and HAAs have been investigated in algal impacted rivers, lakes and resevoirs[9, 10, 30-34] and led to proposals of using chlorophyll *a* as a surrogate measure for the abundance of THM precursors.[10, 30] The algae biomass isolated from the source water of a full-scale drinking water treatment plant during an algal bloom was reported to contribute 20–50% of the total THM and HAA formation.[9] The only study that evaluated N-DBPs (HANs) showed that their formation was higher when the

reservoir organic matter was algal dominated.[33] There is a need to expand research using authentic samples from surface water impacted by algae to evaluate N-DBP formation.

Pre-oxidation is a common strategy for DBP control. Using pure cultures of various algal species, the effects of chlorine, potassium permanganate, ferrate, and ozone have been investigated on THMs, HAAs, chloral hydrate, and, in fewer cases, N-DBPs.[35-41] During an algal bloom, 45% and 60% of the total THM and HAA formation, respectively, was formed during the pre-chlorination stage at the intake to a full-scale treatment plant.[9] A pilot-plant investigated pre-oxidation of eutrophic lake water by ozone, potassium permanganate, chlorine dioxide, and ferrate, observing decreases in chloroform and DCAN, but increases in chloral hydrate, TCNM, and dichloroacetamide.[31] Peracetic acid (PAA) is an emerging disinfectant recently proposed as an algaecide for reservoirs.[42, 43] However, the effect of PAA pre-oxidation on the formation of DBPs has not been evaluated.

The first objective of this study was to assess the DBP risks associated with algal impact. Three algal impacted lakes in Iowa were sampled over a 13-week period in the algal bloom season. The formation of 11 DBPs was monitored under uniform formation conditions (chlorination)[44] and evaluated for correlations with water quality parameters using statistical analyses. The second objective of this study was to investigate the effects of PAA pre-oxidation on DBP formation using field-relevant PAA exposures and algal-impacted surface water samples.

2. Material and Methods

2.1 Materials

Information regarding the chemicals used in this study can be found in Text S1. The peracetic acid (PAA) stock solution was obtained from Sigma Aldrich (32% PAA, 40–45% acetic

acid, <6% hydrogen peroxide (H_2O_2)). The PAA concentration was determined to be 34.07% using iodometric titration.[45]

2.2 Sample Collection

Lake water samples were collected from Brushy Creek Beach (Lake A), Lower Pine Lake Beach (Lake B), and North Twin Lake East Beach (Lake C) in Iowa from mid-July through early-October 2018 (Table 1). Each unique sample tested here was a composite of lake water grab samples taken from three different locations within each beach at three different depths (surface samples taken at depths that corresponded to ankle, knee, and hip heights of sampling personnel). Green Valley Lake (Lake D) water samples were collected from 6 sites (Figure S1) on July 25, 2019. Samples from each site were composites from four depths across the water column; the depths of each site are described in Table S1. All water samples were collected in HDPE bottles (Thermo Scientific, USA), transported to the Iowa State University laboratory on ice and stored at -20 °C until shipped to University at Buffalo. Most samples remained frozen upon arrival at University at Buffalo. Prior to the disinfection experiments, samples were slowly thawed at 4 °C over 72 hours.

2.3 Water Quality Analyses

Nitrate (NO_3-N), nitrite (NO_2-N), and bromide were measured using an ICS-1000 ion chromatography system with an IonPac AS18 column (Dionex, Sunnyvale, CA). Ammonia (NH_3-N) was measured using the Hach salicylate method (Method 8155). Total organic carbon (TOC) and total nitrogen (TN) were measured using a TOC-L/TN analyzer (Shimadzu Corp., Kyoto, Japan). DOC was obtained by filtering samples through a 0.7 μm pre-combusted glass fiber filter prior to TOC analysis. For PAA pre-oxidized samples, an adjusted DOC was calculated by subtracting the DOC contributed by PAA and acetic acid from the total DOC of the sample.

Dissolved organic nitrogen (DON) was calculated as the difference between TN and inorganic nitrogen (NH_3-N, NO_2-N, and NO_3-N). A Cary 60 UV-Vis spectrometer (Agilent, Technologies, Santa Clara, CA) was used to measure solution absorbance at 254 nm, as well as for the colorimetric analyses of NH_3-N, free chlorine, total chlorine, PAA, and H_2O_2 at respective wavelengths. Specific UV absorbance (SUVA) was calculated as the UV absorbance at 254 nm normalized by the DOC. For PAA pre-oxidized samples, SUVA and DBP yields were calculated using the adjusted DOC. Free and total chlorine residuals were measured using Hach methods 8021 and 8167, respectively. Peracetic acid and hydrogen peroxide were measured using Hach method 10290. The detection limit was 0.01 mg/L for NO_3-N, NO_2-N, chloride, and bromide, 0.1 mg/L for TN, DOC, TOC, free and total chlorine, and peracetic acid, 0.03 mg/L for NH_3-N, and 0.05 mg/L for hydrogen peroxide.

Total chlorophyll concentrations of the three lakes sampled in 2018 (Lake A, B, and C) were measured on site using fresh grab samples with a Phyto-PAM-II Multiple Excitation Wavelength Phytoplankton & Photosynthesis Analyzer (Heinz Walz Company, Germany). The reference spectra used for quantification were cyanobacteria, green algae, diatoms/dinoflagellates, and phycoerythrin-type algae. LED lights were activated at multiple wavelengths (440, 480, 540, 590, and 625 nm) with high intensity to measure chlorophyll fluorescence. When the chlorophyll measurement of a sample was high, a zero offset sample was prepared by filtering the same sample through a 0.22 μm syringe filter (Fisher Scientific, USA).

Total chlorophyll concentrations in the lake sampled in 2019 (Lake D) were measured in the water column using a YSI ProDSS Total Algae PC sensor (Xylem Analytics, OH, USA). The peak wavelength of the irradiating light was 470 nm. Real-time data was recorded at 0.5 m intervals

in the water column at each site during sample collection. Chlorophyll concentrations of the samples were calculated by averaging the chlorophyll values of all the depths.

2.4 Uniform Formation Condition (UFC) Test

Samples from Lake A, B, and C were first filtered using a 0.7 μm pre-combusted glass fiber filter. UFC tests were used for the assessment of DBP formation following the procedure described by Summers et al.[44] with slight modification to tighten the range of allowable chlorine residuals in order to improve consistency and reproducibility. Briefly, chlorine demand was first determined using a 10 mL sample buffered to a pH of 8.0 using 2 mM borate buffer in a head-space free amber vial with a PTFE-faced cap. Five doses of chlorine were spiked into the sample and allowed to react for 24 hours in the dark at 20.0 ± 1.0 °C. The five chlorine doses were selected based on:

$$[\mathrm{NaOCl}] = Z \times [\mathrm{DOC}] + \frac{\mathrm{MW_{Cl2}}}{\mathrm{MW_N}}[\mathrm{NH_3\text{-}N}] \quad \text{(eq. 1)}$$

where [NaOCl] (mg/L as Cl_2), [DOC] (mg C/L), [NH_3-N] (mg N/L) are the concentrations of sodium hypochlorite (NaOCl), DOC, and NH_3-N, respectively, MW_{Cl2} and MW_N are the molecular weights of Cl_2 (71 g/mol) and N (14 g/mol), respectively, and Z is a multiplier with values of 1.2, 1.4, 1.6, 1.8 and 2.0. After 24 hours, free chlorine residuals were tested. The chlorine dose yielding a free chlorine residual of 1.0 ± 0.3 mg/L as Cl_2 was then applied to triplicate 30 mL samples buffered at pH 8.0 by borate buffer. Residual chlorine was quenched after 24 h using excess sodium thiosulfate ($Na_2S_2O_3$) before DBPs were analyzed. Table S2 summarizes the chlorine doses used in all UFC tests in this portion of the study.

2.5 Peracetic Acid (PAA) Pre-Oxidation Experiments

The effects of PAA pre-oxidation on DBP formation was investigated on six samples collected from different locations of lake D. Samples were exposed to PAA prior to filtration to

simulate algae treatment in reservoirs/lakes serving as source water. The method development process is described in Text S2. Each 1 L unfiltered sample was first divided into four 250 mL portions. The first portion was filtered immediately, representing the control. The remaining three portions were dosed with PAA under three conditions: initial dose 2 mg/L with contact time 2 h (hereafter referred to as "low"), 6 mg/L with 2 h (med), and 6 mg/L with 6 h (high). These PAA doses and contact times were selected based on a case study conducted for a storage reservoir of secondary wastewater effluents in Modesto County, CA that had high algal activity; 6 mg/L PAA with 6 h contact time was sufficient to reduce the total suspended solid concentration by 37%.[46] The lower doses and contact times were selected to span the range of PAA exposure that is potentially field relevant. PAA residual was measured after the designated contact time and quenched using $Na_2S_2O_3$ at a molar ratio of 0.22:1.0 ($Na_2S_2O_3$:PAA). The PAA exposure was calculated as:

$$\text{PAA Exposure} = \frac{[\text{PAA}]_{\text{Dose}} - [\text{PAA}]_{\text{Residual}}}{2} \times (\text{Contact Time}) \qquad \text{(eq. 2)}$$

where PAA exposure (mg h L^{-1}), $[\text{PAA}]_{\text{Dose}}$ (mg/L), $[\text{PAA}]_{\text{Residual}}$ (mg/L), and contact time (h) is the calculated PAA exposure, the PAA dosed to the sample, the PAA residual measured after the allotted contact time, and the length of the exposure to PAA, respectively. After reaction with PAA, the samples were filtered through a 0.7 μm pre-combusted glass fiber filter, and the H_2O_2 residual and DOC were measured. UFC tests for PAA pre-oxidized samples followed the procedure described in section 2.4, with slight modification to consider the chlorine demand of hydrogen peroxide in the initial dose selection:

$$[\text{NaOCl}] = Z \times [\text{DOC}] + \frac{\text{MW}_{\text{Cl2}}}{\text{MW}_{\text{N}}}[\text{NH}_3] + \frac{\text{MW}_{\text{Cl2}}}{\text{MW}_{\text{H2O2}}}[\text{H}_2\text{O}_2] \qquad \text{(eq. 3)}$$

where [NaOCl] (mg/L as Cl_2), [DOC] (mg C/L), [NH_3-N] (mg N/L), H_2O_2 (mg/L) are the concentrations of NaOCl, DOC, NH_3-N, and H_2O_2 respectively, MW_{Cl2}, MW_N, and MW_{H2O2} are the molecular weights of Cl_2 (71 g/mol), N (14 g/mol), and H_2O_2 (34 g/mol) respectively, and Z is a multiplier with values 0.2, 0.35, 0.5, 0.65, and 0.8. Table S4 summarizes the chlorine doses used in all UFC tests after PAA pre-oxidation.

2.6 Disinfection Byproduct Analysis

Four THMs including trichloromethane (chloroform), dichlorobromomethane (DCBM), dibromochloromethane (DBCM), and tribromomethane (bromoform), four haloacetonitriles (HANs) including DCAN, trichloroacetonitrile (TCAN), bromochloroacetonitrile (BCAN), and dibromoacetonitrile (DBAN), two HKs including 1,1-dichloropropanone (1,1-DCP) and 1,1,1-trichloropropanone (1,1,1-TCP), and one halonitromethane, TCNM, were analyzed. After quenching the residual chlorine with excess $Na_2S_2O_3$, samples were spiked with 1,2-dibromopropane as internal standard and then mixed with 2 mL of methyl tert-butyl ether (MTBE) and 10 g sodium sulfate. The samples were shaken for 2 min and then allowed to rest for 10 min. The MTBE layer was transferred to the gas chromatography instrument with an electron capture detector (GC-ECD, Agilent 7890B-^{63}Ni ECD). The GC-ECD methods are as previously described.[29] The detection limit for all DBPs was 0.1 μg/L.

2.7 Calculation of Cytotoxicity

The cytotoxicity contributed by each DBP was calculated from the ratio of the concentration of DBPs formed in the UFC test and their corresponding median lethal concentration (LC_{50}) determined in a Chinese Hamster ovary (CHO) cell assay.[47] Following a toxicity-weighted approach in previous studies,[48, 49] we used the following calculation to compare cytotoxicity among samples:

$$\text{Cytotoxicity} = \sum_i \frac{[\text{DBP}]_i}{\text{LC}_{50,\text{DBP}_i}} \quad \text{(eq. 4)}$$

where $[DBP]_i$ is the concentration of DBP_i formed in the UFC test (M); $LC_{50,DBPi}$ is the median lethal dose of individual DBPs determined in a CHO cell assay (M).[47] Because LC_{50} values are not available for HKs, they were not included in the cytotoxicity calculations for different samples. The calculated toxicity assumes that the toxicity from individual DBPs is additive, and only accounts for the nine measured DBPs (four THMs, four HANs, and TCNM).

2.8 Statistical Methods

Statistical relationships were evaluated using the Pearson's correlation coefficient (r) and Spearman's rank coefficient (ρ) correlation tests in Minitab 19.2. Pearson's r is a parametric test that measures the degree of linearity between two variables, with $-1 \leq r \leq 1$, and Spearman's ρ is a nonparametric test that measures the degree to which two variables fit a monotonic function, with $-1 \leq \rho \leq 1$. A p-value ≤ 0.05 was used as the cutoff for statistical significance. A strong correlation has the additional criteria of r, $\rho \geq |0.5|$, in addition to $p \leq 0.05$. For the independent variables (e.g., water quality parameters), all values below the detection limit were assigned a value of half of the corresponding detection limit, with the exception of DON, which was calculated from the NH_3-N, NO_3-N, and NO_2-N subtracted from the TN, and not directly measured.

2.9 Excitation Emission Matrix (EEM) Analysis

Fluorescence EEMs were determined using a Cary Eclipse fluorescence spectrophotometer following the published protocol from Chen et al.[50] Samples were first diluted to 1 mg/L DOC, spiked with 0.01 M KCl, and acidified to pH 3 using 2 N HCl. For samples pre-oxidized by PAA, the dilution factor was calculated using the DOC value prior to PAA addition (Text S2). Excitation and emission slits were set to 10 nm band-pass. Excitation wavelengths ranged from 200 nm to

400 nm at 5 nm increments. At each excitation wavelength, the fluorescence was measured at emission wavelengths ranging from 290 nm to 550 nm at 2 nm increments. EEM data was processed using a parallel factor analysis (PARAFAC) model in RStudio (version 1.2.5001) to subtract a blank, correct for the inner-filter effect, and remove interpolate scattering.[51, 52] Processed data was plotted in contour plots in Origin Pro 2020 and volume integrated to evaluate the relative fluorescence intensity of five regions associated with tyrosine-like (I), tryptophan-like (II), fulvic-like (III), soluble microbial product-like (IV), and humic-like (V) moieties.[50]

3. Results and Discussion

3.1 Temporal variability of DBP formation potential in algal impacted waters

Table 1 summarizes the water quality for the samples collected from three Iowa lakes over 13 weeks between July and October 2018. As shown in Figure 1, total chlorophyll concentrations ranged from 2.6–70.5 μg/L in these samples, representing different degrees of algal activity; the low SUVA values for most samples also suggest algal impacts. Only two samples (A7 and B11, Table 1) had SUVA values above 3 L mg^{-1} m^{-1}, suggesting the dissolved organic matter was primarily terrestrially derived. Lake C samples had the highest average total chlorophyll concentrations and lowest SUVA values, indicating that this lake had the highest degree of algal impact.

Figures 2 and S4 show the concentration of DBPs formed in UFC tests for Lake A, B, and C samples and the corresponding calculated cytotoxicity of the samples. For all samples THMs formed in the greatest abundance (90–370 μg/L), followed by HANs (6.5–87 μg/L). Far less HKs (0.4–11.4 μg/L) and TCNM (0.3–9.7 μg/L) were formed. All four species of THMs were detected in 15 of the 26 samples; bromoform was below the detection limit in 11 tests. Among HANs, DCAN and BCAN were detected in all samples, whereas DBAN was only detected in three

samples. When considering the calculated cytotoxicity, HANs contributed 89–99% of the overall toxicity, an order of magnitude greater than THMs (Figures 2b, S4b, and S4d), despite the lower concentration of HANs. All spikes in calculated cytotoxicity of samples (A11, B11, B13, and C9) (Figures 2 and S4) are associated with spikes in HAN formation. A11 and C9 samples had high total chlorophyll concentrations (70.5 and 68.4 μg/L, respectively), suggesting high algal activity; B11 and B13, although had lower than average total chlorophyll concentrations (15.7 and 25.9 μg/L, respectively), had high DOC (12.0 and 5.27 mg C/L, respectively) and DON (4.52 and 0.68 mg N/L, respectively). Figure S5 further shows that the calculated cytotoxicity of the samples correlated with their HAN concentration ($r = 0.990$, $p < 0.001$). B13, with the highest HAN formation, deviated from the linear trend, attributable to the formation of the more toxic HAN species BCAN[47] at a level (5.0 μg/L) greater than other samples (0.35–1.56 μg/L). Although HKs were not included in the cytotoxicity calculation due to the lack of LC_{50} values from the CHO cell bioassay, they are not expected to be main contributors to toxicity as shown in a previous study.[49] Our observation that HANs are a main cytotoxicity driver is consistent with those in previous studies.[15, 49, 53, 54]

The temporal trends (Figure 3) and variability (Figure S6) of DBP yields can indicate the difference in the source and composition of organic matter over the algal bloom season. For example, it is observed that HAN yields significantly increased in concentration in week 11 for Lakes A and B while THM yields remained constant, indicating a shift in DBP precursors compared with the other sampling weeks. THMs and HANs varied by the greatest magnitude during the sampling period, ranging from 14–36 μg/mg C and 1.0–17 μg/mg C, respectively. However, the greatest fold-difference was observed with TCNM (0.04–2.3 μg/mg C), which can be attributed to the low TCNM formation in Lake C (0.06–0.29 μg/mg C, further discussed in

section 3.2). Correlation analysis (Table S6) on the aggregated data showed that the yields of THMs correlated with those of the other three DBP groups. AOM was previously reported to have greater HAN yields and smaller THM yields than allochthonous organic matter,[11] which would suggest that spikes in HAN yields can be accompanied by drops in THM yields during algal blooms. This, however, was not observed in our results. On the other hand, the correlation in the aggregated data between the yields of THMs and other DBPs suggests that despite the low contribution of THMs to overall cytotoxicity, this group of regulated (and hence routinely monitored) DBP may be useful for predicting the overall DBP risk for waters with moderate algal impact. When inspecting the correlation between the yields of THMs and other DBPs in individual lakes (Table S6), however, correlation was not found for Lake C. Among the three lakes, Lake C had the highest total chlorophyll concentrations (average level 44 μg/L) and lowest SUVA (average level 1.81 L mg^{-1} m^{-1}) (Figure 1) indicating that lake had the highest algal activity and that the dissolved organic matter was algal dominated. These results suggest that the use of THM yields as an indicator for other DBP yields should be cautioned for waters with extremely high algal impact.

3.2 Correlation between DBP formation and water quality parameters

Figures 1 and S7 show the variability in water quality for Lake A, B, and C samples, the values for which are shown in Table 1. The relationship between the yields of DBPs in UFC tests and water quality parameters of the samples, including total chlorophyll, SUVA, NO_2-N, NO_3-N, NH_3-N, DON, and DOC were evaluated (Table 2). All correlation tests, except the ones with DOC as the independent variable, were evaluated using DBP yields (i.e., DOC-normalized DBP concentrations) to shed light on the source of organic carbon in the samples, because AOM was previously reported to have greater N-DBP yields and smaller THM yields than NOM.[11]

Chlorophyll is a common indicator of algal blooms.[10, 30, 55, 56] Total chlorophyll concentrations in samples from Lake A, B, and C ranged from 2.6–71 μg/L (Table 1, Figure 1), representing different degrees of algal activity. If AOM were the primary contributor of N-DBP precursors, total chlorophyll could be used as an indicator of N-DBP risk. However, over the 13-week period of this study, no correlation (in each lake or the aggregated data) was observed between total chlorophyll concentrations and DBP yields (Table 2 and Figure 4). Neither did the non-DOC-normalized DBP concentrations correlate with total chlorophyll concentrations (Table 2 and Figure S8). These results suggest that total chlorophyll would not be a suitable surrogate parameter for the measurement of N-DBP precursors. A previous study proposed that a chlorophyll *a* standard could help limit THM formation in drinking water treatment plants, based on a THM/chlorophyll *a* relationship indirectly derived from the relationship between high algal activity and chlorophyll *a*, low SUVA, and low TOC removal.[10] Another study reported a correlation between chlorophyll *a* and THM concentrations,[30] but it may be attributed to two factors: first, high chlorine dose and long contact time (i.e., 3.0–5.0 mg/L Cl_2 residual after 7 d exposure) was used in contrast to the UFC test in our study that approximates chlorination conditions relevant to drinking water disinfection (i.e., 1.0 ± 0.3 mg/L as Cl_2 residual after 24 h exposure); second, the seasonal average of chlorophyll *a* concentrations were used in the correlation analysis in contrast to the chlorophyll concentrations of the individual samples used in our study.

The yields of TCNM correlated with both NO_2-N ($p = 0.005$) and NO_3-N ($p < 0.001$) concentrations in the samples (Table 2, Figures S9 and S10). The NO_2-N concentrations of all Lake C samples were below the detection limit (0.01 mg N/L); correspondingly, only 0.1–0.3 μg/mg C of TCNM was formed. In comparison, Lake A had much higher levels of NO_2-N (< 0.01–

0.24 mg N/L), and correspondingly yielded 1.0 – 2.3 μg/mg C of TCNM. Previous studies have observed the promotion of TCNM formation by nitrite. For example, the addition of 2 mg N/L NO_2^- to a raw water sample increased TCNM formation in UFC tests by more than three-fold (from < 0.18 μg/mg C to 0.71 μg/mg C).[28] Similarly, the presence of 1 mg N/L NO_2^- during chlorination increased the formation of TCNM by 50% for a sample containing intracellular algal organic matter and by 210% and 450% for two samples containing terrestrially-derived organic matter.[57] Additionally, NO_2^- was shown to form additional TCNM precursors through nitration under sunlight.[29] The relationship between NO_3-N and TCNM yields is likely explained by the strong multicollinearity between NO_2-N and NO_3-N ($r = 0.773$, $p < 0.001$).

SUVA correlated with the yields of THMs, TCNM and HKs, but not HANs (Table 2, Figure S11). SUVA is an indicator of the aromaticity of organic matter. Previous studies showed that organic matter in samples with SUVA < 2 L mg^{-1} m^{-1} are autochthonous, while those with SUVA > 3 L mg^{-1} m^{-1} are allochthonous.[8, 10, 33, 57] SUVA values for Lake A, B and C samples ranged from 1.25–5.40 L mg^{-1} m^{-1} (Table 1), representing different degrees of algal and terrestrial-dominated organic matter in the samples. Our observation that SUVA correlates with THMs and TCNM, but not HANs, are consistent with the findings of previous studies on DBP formation in various surface/source waters.[10, 58-61] THM yields correlated with the SUVA values in a survey of drinking water reservoirs;[10] THM and TCNM yields correlated with SUVA values in 21 NOM isolates from three source waters.[58]

DON was observed to correlate with the yields of both HANs and HKs (Table 2, Figure S12). This is consistent with previous reports that DON is an essential precursor for the formation of HANs.[61-65] For ten extracted fulvic and humic substances, the formation potential of DCAN, the most abundant HAN, was found to correlate with the DON content.[64] Chen and Westerhoff

also reported that their HAN predictive model based on DOC, UV_{254} and bromide was significantly improved after the inclusion of DON as an independent variable.[66]

DOC correlated positively with the non-normalized formation of THMs, HANs, and HKs (Table 2, Figure S13). Consistent with our findings, DOC was shown to correlate with the formation of THMs upon chlorination of various water sources.[30, 34, 67, 68] Correlations were observed between the mean epilimnetic DOC and THM formation potential of 21 lakes and reservoirs in New York,[30] and between DOC in 24 source water samples and THM levels in the finished water of the drinking water treatment plants.[67] In addition, DOC was previously found to be an important component in predictive models for the formation of chloroform and HANs in samples from drinking water treatment plants, wastewater treatment plants, and jar tests.[66] A negative correlation was observed between DOC and TCNM in Spearman's test. However, this may be an artifact introduced by the samples from Lake C, which has very little TCNM formation (likely due to the low nitrite concentrations as discussed earlier) but higher than average DOC concentrations compared to Lakes A and B.

While the above correlation analysis yields general observations across algal-impacted waters, temporal dynamic of the samples is also worth considering. The most distinct case is the two consecutive samples B11 and B13. These two samples had the greatest concentrations/yields of HANs among all samples were formed in samples B11 (81.2 μg/L and 6.8 μg/mg C for B11; 87.2 μg/L and 16.6 μg/mg C for B13) (Table S5). Over the two-week sampling interval, the water quality shifted drastically. B11 contained high DOC (12.0 mg C/L) and DON (4.52 mg N/L), as well as high SUVA (5.40 L mg^{-1} m^{-1}) and low total chlorophyll (15.7 μg/l), indicating low algal activity and terrestrially-dominated organic matter. B13, collected two weeks after B11, had lower DOC (5.27 mg C/L) and DON (0.68 mg N/L), but higher total chlorophyll (25.9 μg/L) and lower

SUVA (1.85 L mg^{-1} m^{-1}) suggesting that algal activity increased and that organic matter shifted from terrestrially to algal-dominated. This accompanied the increase in HAN formation, potentially attributed to a subset of high-yield nitrogenous precursors in the algal-derived organic matter.

3.3 Effects of Peracetic Acid Pre-Oxidation

The effects of PAA pre-oxidation on the formation of DBPs in subsequent chlorination (UFC test) was evaluated using six samples collected at different locations of a eutrophic lake (Lake D) on July 25, 2019. Samples were exposed to PAA for designated contact time, filtered, and then subject to UFC test. Figure 5 shows the difference in the amount of DBPs formed in the UFC tests between PAA pre-oxidized samples and their controls. The formation of THMs was reduced in 80% of the samples by PAA pre-oxidation, especially at high exposure. With an initial PAA dose of 6 mg/L with contact time 6 h (exposure 23.8–28.7 mg h L^{-1}), THM formation was reduced by 8.7–61.5 μg/L. In contrast, the formation of HANs, TCNM, and HKs was promoted by PAA pre-oxidation in a significant portion (70%, 50%, and 40%, respectively) of the samples, although the change was not dose-dependent. No PAA pre-oxidized samples showed lower formation of TCNM or HKs; only one PAA pre-oxidized sample showed lower HAN formation.

Figure 6 shows the percent change in calculated cytotoxicity between PAA pre-oxidized samples and the corresponding controls. For approximately half of the samples, PAA pre-oxidation increased the calculated cytotoxicity. Specifically, for samples D4 and D6, PAA pre-oxidation increased the calculated cytotoxicity across all three PAA exposures. These results suggest that PAA pre-oxidation could increase the cytotoxicity of the finished water as an unintended consequence, and therefore the specific source water should be evaluated prior to the adoption of PAA for reservoir algal control.

The influence of PAA pre-oxidation on the DBP yields in the subsequent UFC tests is shown in Figure S15. For PAA pre-oxidized samples, the yield was calculated as the concentration of DBPs formed in the UFC test, divided by the adjusted DOC (the DOC contributed by PAA and acetic acid was subtracted from the measured DOC of the pre-oxidized sample). The yields of THMs and HANs decreased in more than 80% of the PAA pre-oxidized samples; greater decrease in yields was observed with greater PAA exposure, except for D4 and D5. The yields of TCNM were reduced by PAA pre-oxidation in about 50% of the samples and increased in only one sample. The yields of HKs were not statistically different from their corresponding control in 60% of the samples, and increased in 30% of the samples. The change in the yields of TCNM and HKs by PAA pre-oxidation was generally not dose-dependent with PAA exposure.

The observed change in DBP formation by PAA pre-oxidation is likely due to the change in the concentration and composition of organic matter. The lake water samples used in this study contained a mixture of particulate and dissolved organic matters with both allochthonous and autochthonous origins. Allochthonous organic matter was previously shown to have higher THM yields but lower N-DBP yields than AOM.[11] Furthermore, IOM has greater N-DBP yields than EOM.[12] Two coincident pathways can occur during PAA pre-oxidation: (1) the release of new dissolved organic matter from particulate organic matter (e.g., lysis of algal cells) by PAA and (2) oxidation of dissolved organic matter by PAA. Accordingly, DOC, DON, and SUVA were monitored for all samples (Table 3) and fluorescence EEMs were generated for samples D3–D6 (Figure 7 for sample D6 as an example). After PAA pre-oxidation, DOC increased in all samples (after subtracting the DOC contributed by PAA and acetic acid in the stock solution); higher PAA exposure generally resulted in greater increase in DOC concentration. The increase in DOC by PAA pre-oxidation is similar to that observed after pre-oxidation of algal suspensions by

chlorination,[36, 37] potassium permanganate,[36, 69] UV irradiation,[70] ozone,[38, 41, 71] and chlorine dioxide.[72] DON also increased after PAA pre-oxidation, whereas SUVA values decreased for most samples. These results suggest that PAA exposure released dissolved organic matter from particulates, contributing to the pool of DBP precursors and that these new organic materials are autochthonous in nature, such as the IOM of algae. Increase in DON was also observed after pre-chlorination[37] and pre-ozonation[41] of a suspension of *Microcystis aeruginosa* cells. As discussed previously (section 3.2), DOC correlated with the concentrations of THMs, HANs, and HKs formed in UFC tests across different lake samples, DON correlated with the yields of HANs and HKs, and SUVA correlated with the yields of THMs, TCNM, and HKs. After PAA pre-oxidation, two thirds of the samples exhibiting an increase in DON concentration also showed an increase in HAN formation in the UFC test. In addition, the increase in DOC and decrease in THM formation after PAA pre-oxidation seemingly contradict the positive correlation between the two observed using different lake samples (section 3.2). This can be attributed to the change in the composition of dissolved organic matter as suggested by the lower SUVA values after PAA pre-oxidation and the fluorescence EEM analysis discussed below. Consistent with our findings in section 3.2 the change in SUVA by PAA pre-oxidation correlated with the change in the yields of THMs and TCNM (Figure S16). However, the change in HAN yields also correlated well, but not HKs.

The change in organic matter composition by PAA pre-oxidation is supported by the change in the fluorescence EEMs of the samples (Figures 7 and 8). The five regions in the EEMs (I–V) correspond to tyrosine-like, tryptophan-like, fulvic-like, soluble microbial product-like, and humic-like substances, respectively. Decreases in the fluorescence intensity were commonly observed at low and high PAA exposure for all regions, which is consistent with the oxidative transformation of dissolved organic matter. Other oxidation treatment methods such as UV

irradiation, ozonation, and advanced oxidation (UV/H_2O_2 and UV/peroxydisulfate) on dissolved AOM solutions were also found to reduce the overall fluorescence intensity.[70, 73-75] On the other hand, with medium PAA exposure, our observations were less consistent. D6 exhibited as high as 65% and 96% increases in the fluorescence intensity of tyrosine- and tryptophan-like regions, respectively; D4 also exhibited 33% and 32% increases in these two regions, respectively. This phenomenon is best visualized for sample D6 in Figure 7, where an increase in fluorescence in the tyrosine-like and tryptophan-like regions was only observed under medium PAA exposure. Considering that IOM is rich in aromatic proteins that fluoresce in tyrosine- and tryptophan-like regions,[12] these results further support that dissolved organic matter was released from particulates, including suspended algal cells. Out of the four samples (D3–D6), D6 had the highest algal activity based on its total chlorophyll concentration; accordingly, the increase in its fluorescence signals was generally greater than other samples. The change in fluorescence by PAA pre-oxidation shares similarities with those observed for other pre-oxidation methods. Pre-ozonation of exponential-phase *Microcystis aeruginosa* cells at low ozone dose (0.5 mg/L) was shown to substantially increase the intensity in the soluble microbial product-like region and slightly increase the intensity in the tyrosine- and tryptophan-like regions, but this trend diminished and eventually reversed at higher ozone doses (1–4 mg/L).[41] This was explained by the release of dissolved organic matter from algal cell lysis at low ozone doses and the further degradation of the original and newly released dissolved organic matter upon higher ozone exposure. The same general trend was observed for PAA at medium and high exposure in D4 and D6. They both exhibited increases in the intensity of tyrosine, tryptophan-, fulvic-, and soluble microbial product-like regions at medium PAA exposure (8.4–10.5 mg h L^{-1}), but decreases in these regions at higher PAA exposure

(23.8–28.2 mg h L^{-1}). The higher concentration/exposure of PAA than ozone is consistent with the weaker oxidation strength of PAA.

The change in fluorescence signals by PAA partially explains the change in DBP formation. The formation potential of THMs was previously reported to correlate with the fluorescence intensity in the humic-like and fulvic-like regions of EEMs.[59, 72, 76, 77] Generally, we observe a decrease in the fluorescence intensity of these regions after PAA pre-oxidation. Correspondingly, THMs decreased in 80% of the samples. Exception was observed for D4 and D6 after medium exposure to PAA, for which THM formation decreased but fluorescence intensity increased. The formation of HANs was higher in 70% of the samples after PAA pre-oxidation despite the general decrease in the intensity of tyrosine- and tryptophan-like regions, which was reported to correlate with the formation potential of DCAN and BCAN[78] and correspond to the decrease in DCAN formation potential when removed by treatment (e.g., biological activated carbon)[79] or natural processes (e.g., sunlight irradiation)[80]. It should be noted however, that these HAN studies used high chlorine dose (15–170 mg/L as Cl_2) to force almost all precursors to form DBPs, in contrast to the UFC test conditions in this study that are closer to drinking water disinfection. The mixed nature of organic matter in our samples, including both autochthonous and allochthonous organic materials, can results in competition between precursors. Algae-derived, reactive HAN/TCNM precursors by PAA pre-oxidation may outcompete THM precursors in reacting with chlorine in the UFC test.

4. Conclusions

In this study we assessed the DBP risks of algal impacted surface waters and the impacts of PAA pre-oxidation on DBP risks. Using UFC tests, we found that although THMs formed in the greatest abundance, the HANs contributed to most of the calculated cytotoxicity (89–99%),

such that the formation of HANs was strongly correlated with toxicity ($r = 0.990$, $p < 0.001$). A positive correlation between the yields of THMs and those of other DBPs suggest that the routinely monitored THMs may be used as an indicator for unregulated, but more toxic DBPs. Contrary to our expectation, total chlorophyll, a common indicator of algal activities, did not correlate with DBP yields. Inorganic nitrogen species nitrite and nitrate both correlated with the yields of TCNM, whereas DON correlated with the yields of HANs. DOC and SUVA correlated with the non-normalized formation of DBPs (μg/L) and DBP yields (μg/mg C), respectively.

The effects of PAA pre-oxidation differed among DBPs. PAA pre-oxidation promoted the formation of HANs and TCNM in 70% and 50% of samples, respectively, in the subsequent UFC test, but reduced the formation of THMs in 80% of the samples. On the other hand, the yields of THMs, HANs, and TCNM decreased in 90%, 80%, and 50% of samples, respectively. Approximately half of the PAA pre-oxidized samples showed higher cytotoxicity compared with their control. In other words, although PAA pre-oxidation may help with THM compliance, it can potentially lead to higher toxicity of the finished water. Thus, it is recommended that utilities conduct thorough evaluations before deciding to use PAA for algal control. The change in DOC, DON, SUVA, and fluorescence EEMs suggest that PAA served dual roles. On one hand, PAA oxidation releases organic matter from particulates and thereby increased the pool of DBP precursors. On the other hand, PAA, especially at high exposure, also contributed to oxidative transformation of dissolved organic matter, some of which resulted in the degradation of DBP precursors.

Supporting Information

Additional Information on materials and method development, supporting data in the form of tables and figures, and numeric data for the figures in the main text are available in the Supporting Information.

Conflicts of Interest

There are no conflicts to declare.

Acknowledgements

This research was supported in part by a grant from the National Science Foundation (CBET 1652412) and a grant from the U.S. Environmental Protection Agency's Science to Achieve Results (STAR) program under Assistance Agreement Number 83927001. The authors would like to thank the Iowa Department of Natural Resources, Elizabeth Swanner, and Grace Wilkinson for assistance in sample collection and in-field chlorophyll data collection.

References:

1. W. Li, X. Xu, J. Yao, N. Tanaka, O. Nishimura and H. Ma, Combined effects of elevated carbon dioxide and temperature on phytoplankton-zooplankton link: A multi-influence of climate change on freshwater planktonic communities, *Science of The Total Environment*, 2019, **658**, 1175-1185.
2. Y. Q. Ding, H. Xu, J. M. Deng, B. Q. Qin and Y. W. He, Impact of nutrient loading on phytoplankton: a mesocosm experiment in the eutrophic Lake Taihu, China, *Hydrobiologia*, 2019, **829**, 167-187.
3. J. M. O'Neil, T. W. Davis, M. A. Burford and C. J. Gobler, The rise of harmful cyanobacteria blooms: The potential roles of eutrophication and climate change, *Harmful Algae*, 2012, **14**, 313-334.
4. W. W. Carmichael, Health effects of toxin-producing cyanobacteria: "The CyanoHABs", *Hum. Ecol. Risk Assess.*, 2001, **7**, 1393-1407.
5. S. B. Watson, J. Ridal and G. L. Boyer, Taste and odour and cyanobacterial toxins: impairment, prediction, and management in the Great Lakes, *Can. J. Fish. Aquat. Sci.*, 2008, **65**, 1779-1796.
6. Y. Zhang, M. A. van Dijk, M. Liu, G. Zhu and B. Qin, The contribution of phytoplankton degradation to chromophoric dissolved organic matter (CDOM) in eutrophic shallow lakes: Field and experimental evidence, *Water Research*, 2009, **43**, 4685-4697.
7. N. Her, G. Amy, H. R. Park and M. Song, Characterizing algogenic organic matter (AOM) and evaluating associated NF membrane fouling, *Water Research*, 2004, **38**, 1427-1438.

8. E. H. Goslan, C. Seigle, D. Purcell, R. Henderson, S. A. Parsons, B. Jefferson and S. J. Judd, Carbonaceous and nitrogenous disinfection by-product formation from algal organic matter, *Chemosphere*, 2017, **170**, 1-9.
9. C. Chen, X.-j. Zhang, L.-x. Zhu, J. Liu, W.-j. He and H.-d. Han, Disinfection by-products and their precursors in a water treatment plant in North China: Seasonal changes and fraction analysis, *Science of the Total Environment*, 2008, **397**, 140-147.
10. J. F. Saunders, A. K. Hohner, R. S. Summers and F. L. Rosario-Ortiz, Regulating Chlorophyll a to Control DBP Precursors in Water Supply Reservoirs, *Journal: American Water Works Association*, 2015, **107**, E603-E612.
11. J. Fang, J. Ma, X. Yang and C. Shang, Formation of carbonaceous and nitrogenous disinfection by-products from the chlorination of Microcystis aeruginosa, *Water Research*, 2010, **44**, 1934-1940.
12. J. Fang, X. Yang, J. Ma, C. Shang and Q. Zhao, Characterization of algal organic matter and formation of DBPs from chlor(am)ination, *Water Research*, 2010, **44**, 5897-5906.
13. H. Sun, X. Song, T. Ye, J. Hu, H. Hong, J. Chen, H. Lin and H. Yu, Formation of disinfection by-products during chlorination of organic matter from phoenix tree leaves and Chlorella vulgaris, *Environmental Pollution*, 2018, **243**, 1887-1893.
14. J. Huang, N. Graham, M. R. Templeton, Y. Zhang, C. Collins and M. Nieuwenhuijsen, A comparison of the role of two blue–green algae in THM and HAA formation, *Water Research*, 2009, **43**, 3009-3018.
15. M. G. Muellner, E. D. Wagner, K. McCalla, S. D. Richardson, W. Yin-Tak and M. J. Plewa, Haloacetonitriles vs. Regulated Haloacetic Acids: Are Nitrogen-Containing DBPs More Toxic?, *Environmental Science & Technology*, 2007, **41**, 645-651.
16. M. J. Plewa, E. D. Wagner, M. G. Muellner, K.-M. Hsu and S. D. Richardson, in *Disinfection By-Products in Drinking Water*, American Chemical Society, 2008, vol. 995, ch. 3, pp. 36-50.
17. L.-C. Hua, J.-L. Lin, P.-C. Chen and C. Huang, Chemical structures of extra- and intra-cellular algogenic organic matters as precursors to the formation of carbonaceous disinfection byproducts, *Chemical Engineering Journal*, 2017, **328**, 1022-1030.
18. J. Chen, N. Gao, L. Li, M. Zhu, J. Yang, X. Lu and Y. Zhang, Disinfection by-product formation during chlor(am)ination of algal organic matters (AOM) extracted from Microcystis aeruginosa: effect of growth phases, AOM and bromide concentration, *Environmental Science & Pollution Research*, 2017, **24**, 8469-8478.
19. S. Zhou, Y. Shao, N. Gao, Y. Deng, L. Li, J. Deng and C. Tan, Characterization of algal organic matters of Microcystis aeruginosa: Biodegradability, DBP formation and membrane fouling potential, *Water Research*, 2014, **52**, 199-207.
20. Z. M. Zhao, W. J. Sun, A. K. Ray, T. Mao and M. B. Ray, Coagulation and disinfection by-products formation potential of extracellular and intracellular matter of algae and cyanobacteria, *Chemosphere*, 2020, **245**, 9.
21. F. Dong, Q. Lin, C. Li and T. Zhang, Evaluation of disinfection byproduct formation from extra- and intra-cellular algal organic matters during chlorination after Fe(vi) oxidation, *RSC Advances*, 2019, **9**, 41022-41030.
22. T. W. Davis, D. L. Berry, G. L. Boyer and C. J. Gobler, The effects of temperature and nutrients on the growth and dynamics of toxic and non-toxic strains of Microcystis during cyanobacteria blooms, *Harmful Algae*, 2009, **8**, 715-725.
23. X. F. Yang, X. Zheng, L. J. Wu, X. Cao, Y. Li, J. F. Niu and F. G. Meng, Interactions between algal (AOM) and natural organic matter (NOM): Impacts on their photodegradation in surface waters, *Environmental Pollution*, 2018, **242**, 1185-1197.

24. M. Pivokonsky, J. Naceradska, T. Brabenec, K. Novotna, M. Baresova and V. Janda, The impact of interactions between algal organic matter and humic substances on coagulation, *Water Research*, 2015, **84**, 278-285.
25. D. T. Myat, M. B. Stewart, M. Mergen, O. Zhao, J. D. Orbell and S. Gray, Experimental and computational investigations of the interactions between model organic compounds and subsequent membrane fouling, *Water Research*, 2014, **48**, 108-118.
26. G. S. Bullerjahn, R. M. McKay, T. W. Davis, D. B. Baker, G. L. Boyer, L. V. D'Anglada, G. J. Doucette, J. C. Ho, E. G. Irwin, C. L. Kling, R. M. Kudela, R. Kurmayer, A. M. Michalak, J. D. Ortiz, T. G. Otten, H. W. Paerl, B. Q. Qin, B. L. Sohngen, R. P. Stumpf, P. M. Visser and S. W. Wilhelm, Global solutions to regional problems: Collecting global expertise to address the problem of harmful cyanobacterial blooms. A Lake Erie case study, *Harmful Algae*, 2016, **54**, 223-238.
27. Y. W. Chen, B. Q. Qin, K. Teubner and M. T. Dokulil, Long-term dynamics of phytoplankton assemblages: Microcystis-domination in Lake Taihu, a large shallow lake in China, *J. Plankton Res.*, 2003, **25**, 445-453.
28. J. Hu, H. Song and T. Karanfil, Comparative Analysis of Halonitromethane and Trihalomethane Formation and Speciation in Drinking Water: The Effects of Disinfectants, pH, Bromide, and Nitrite, *Environmental Science & Technology*, 2010, **44**, 794-799.
29. J. Xu, Z. T. Kralles and N. Dai, Effects of Sunlight on the Trichloronitromethane Formation Potential of Wastewater Effluents: Dependence on Nitrite Concentration, *Environmental science & technology*, 2019, DOI: 10.1021/acs.est.9b00447.
30. C. W. Callinan, J. P. Hassett, J. B. Hyde, R. A. Entringer and R. K. Klake, Proposed nutrient criteria for water supply lakes and reservoirs, *J. Am. Water Work Assoc.*, 2013, **105**, 47-48.
31. J. Hu, W. Chu, M. Sui, B. Xu, N. Gao and S. Ding, Comparison of drinking water treatment processes combinations for the minimization of subsequent disinfection by-products formation during chlorination and chloramination, *Chemical Engineering Journal*, 2018, **335**, 352-361.
32. J. Jack, T. Sellers and P. A. Bukaveckas, Algal production and trihalomethane formation potential: an experimental assessment and inter-river comparison, *Canadian Journal of Fisheries & Aquatic Sciences*, 2002, **59**, 1482.
33. R. Zhao, D. A. Reckhow, W. C. Becker and S. Schindler, Seasonal Variation of Disinfection Byproduct Precursors in a Large Water Supply, *Journal: American Water Works Association*, 2018, **110**, 15-32.
34. M.-L. Nguyen, L. A. Baker and P. Westerhoff, DOC and DBP precursors in western US watersheds and reservoirs, *Journal - American Water Works Association*, 2002, **94**, 98-112.
35. S. Zhou, S. Zhu, Y. Shao and N. Gao, Characteristics of C-, N-DBPs formation from algal organic matter: Role of molecular weight fractions and impacts of pre-ozonation, *Water Research*, 2015, **72**, 381-390.
36. X. Shi, R. Bi, B. Yuan, X. Liao, Z. Zhou, F. Li and W. Sun, A comparison of trichloromethane formation from two algae species during two pre-oxidation-coagulation-chlorination processes, *Science of the Total Environment*, 2019, **656**, 1063-1070.
37. J. Qi, H. Lan, R. Liu, S. Miao, H. Liu and J. Qu, Prechlorination of algae-laden water: The effects of transportation time on cell integrity, algal organic matter release, and chlorinated disinfection byproduct formation, *Water Research*, 2016, **102**, 221-228.
38. J. D. Plummer and J. K. Edzwald, Effect of ozone on disinfection by-product formation of algae, *Water Science and Technology*, 1998, **37**, 49-55.
39. M. Ma, M. Wang, X. Cao, Y. Li and J. Gu, Yield of trihalomethane, haloacetic acid and chloral upon chlorinating algae after coagulation-filtration: Is pre-oxidation necessarily negative for disinfection by-product control?, *Journal of Hazardous Materials*, 2019, **364**, 762-769.

40. F. L. Dong, J. Q. Liu, C. Li, Q. F. Lin, T. Q. Zhang, K. J. Zhang and V. K. Sharma, Ferrate(VI) pre-treatment and subsequent chlorination of blue-green algae: Quantification of disinfection byproducts, *Environ. Int.*, 2019, **133**, 8.
41. A. Tang, X. Shi, R. Bi, X. Liao, J. Zou, W. Sun and B. Yuan, Effects of pre-ozonation on the cell characteristics and N-nitrosodimethylamine formation at three growth phases of Microcystis aeruginosa, *Environmental Science and Pollution Research*, 2020, **27**, 873-881.
42. R. K. Chhetri, A. Baun and H. R. Andersen, Algal toxicity of the alternative disinfectants performic acid (PFA), peracetic acid (PAA), chlorine dioxide (ClO2) and their by-products hydrogen peroxide (H2O2) and chlorite (ClO2-), *Int. J. Hyg. Environ. Health.*, 2017, **220**, 570-574.
43. J. F. Kramer, Peracetic acid: A new biocide for industrial water applications, *Mater. Perform.*, 1997, **36**, 42-50.
44. R. S. Summers, S. M. Hooper, H. M. Shukairy, G. Solarik and D. Owen, Assessing DBP yield: uniform formation conditions, *Journal - American Water Works Association*, 1996, **88**, 80-93.
45. A. American Public Health, *Standard Methods for the Examination of Water and Wastewater*, Boston, 1915.
46. Enviro Tech Chemicals Inc., *Control of Pond Algae Utilizing Peracetic Acid - City of Modesto, CA*, Modesto, CA, 2003.
47. E. D. Wagner and M. J. Plewa, CHO cell cytotoxicity and genotoxicity analyses of disinfection by-products: An updated review, *Journal of Environmental Sciences*, 2017, **58**, 64-76.
48. Y.-H. Chuang, A. Szczuka and W. A. Mitch, Comparison of Toxicity-Weighted Disinfection Byproduct Concentrations in Potable Reuse Waters and Conventional Drinking Waters as a New Approach to Assessing the Quality of Advanced Treatment Train Waters, *Environmental Science & Technology*, 2019, **53**, 3729-3738.
49. M. J. Plewa, E. D. Wagner and S. D. Richardson, TIC-Tox: A preliminary discussion on identifying the forcing agents of DBP-mediated toxicity of disinfected water, *Journal of Environmental Sciences*, 2017, **58**, 208-216.
50. W. Chen, P. Westerhoff, J. A. Leenheer and K. Booksh, Fluorescence Excitation−Emission Matrix Regional Integration to Quantify Spectra for Dissolved Organic Matter, *Environmental Science & Technology*, 2003, **37**, 5701-5710.
51. K. R. Murphy, C. A. Stedmon, D. Graeber and R. Bro, Fluorescence spectroscopy and multi-way techniques. PARAFAC, *Analytical Methods*, 2013, **5**, 6557-6566.
52. M. Pucher, D. Graeber, S. Preiner and R. Pinto, staRdom: PARAFAC Analysis of EEMs from DOM.*Journal*, 2019.
53. M. J. W. Plewa, Elizabeth D., *Mammalian Cell Cytotoxicity and Genotoxicity of Disinfection By-products*, Denver, CO, 2009.
54. S. S. Lau, X. Wei, K. Bokenkamp, E. D. Wagner, M. J. Plewa and W. A. Mitch, Assessing Additivity of Cytotoxicity Associated with Disinfection Byproducts in Potable Reuse and Conventional Drinking Waters, *Environmental Science & Technology*, 2020, DOI: 10.1021/acs.est.0c00958.
55. S. R. Carpenter, J. J. Cole, M. L. Pace, R. Batt, W. A. Brock, T. Cline, J. Coloso, J. R. Hodgson, J. F. Kitchell, D. A. Seekell, L. Smith and B. Weidel, Early Warnings of Regime Shifts: A Whole-Ecosystem Experiment, *Science*, 2011, **332**, 1079-1082.
56. W. W. Walker, SIGNIFICANCE OF EUTROPHICATION IN WATER-SUPPLY RESERVOIRS, *J. Am. Water Work Assoc.*, 1983, **75**, 38-42.
57. H. C. Hong, L. Y. Qian, Z. Q. Xiao, J. Q. Zhang, J. R. Chen, H. J. Lin, H. Y. Yu, L. G. Shen and Y. Liang, Effect of nitrite on the formation of halonitromethanes during chlorination of organic matter from different origin, *J. Hydrol.*, 2015, **531**, 802-809.

58. G. H. Hua, D. A. Reckhow and I. Abusallout, Correlation between SUVA and DBP formation during chlorination and chloramination of NOM fractions from different sources, *Chemosphere*, 2015, **130**, 82-89.
59. A. D. Pifer and J. L. Fairey, Improving on SUVA(254) using fluorescence-PARAFAC analysis and asymmetric flow-field flow fractionation for assessing disinfection byproduct formation and control, *Water Research*, 2012, **46**, 2927-2936.
60. J. K. Edzwald, W. C. Becker and K. L. Wattier, SURROGATE PARAMETERS FOR MONITORING ORGANIC-MATTER AND THM PRECURSORS, *J. Am. Water Work Assoc.*, 1985, **77**, 122-132.
61. W. Lee, P. Westerhoff and J.-P. Croué, Dissolved Organic Nitrogen as a Precursor for Chloroform, Dichloroacetonitrile, N-Nitrosodimethylamine, and Trichloronitromethane, *Environmental Science & Technology*, 2007, **41**, 5485-5490.
62. P. Westerhoff and H. Mash, Dissolved organic nitrogen in drinking water supplies: a review, *J. Water Supply Res Technol.-Aqua*, 2002, **51**, 415-448.
63. D. A. Reckhow, T. L. Platt, A. L. MacNeill and J. N. McClellan, Formation and degradation of dichloroacetonitrile in drinking waters, *J. Water Supply Res Technol.-Aqua*, 2001, **50**, 1-13.
64. D. A. Reckhow, P. C. Singer and R. L. Malcolm, Chlorination of humic materials: byproduct formation and chemical interpretations, *Environmental Science & Technology*, 1990, **24**, 1655-1664.
65. A. D. Shah and W. A. Mitch, Halonitroalkanes, Halonitriles, Haloamides, and N-Nitrosamines: A Critical Review of Nitrogenous Disinfection Byproduct Formation Pathways, *Environmental Science & Technology*, 2012, **46**, 119-131.
66. B. Chen and P. Westerhoff, Predicting disinfection by-product formation potential in water, *Water Research*, 2010, **44**, 3755-3762.
67. C. H. Xue, Q. Wang, W. H. Chu and M. R. Templeton, The impact of changes in source water quality on trihalomethane and haloacetonitrile formation in chlorinated drinking water, *Chemosphere*, 2014, **117**, 251-255.
68. S. C. Chapra, R. P. Canale and G. L. Amy, Empirical models for disinfection by-products in lakes and reservoirs, *J. Environ. Eng.-ASCE*, 1997, **123**, 714-715.
69. L. Wang, J. L. Qiao, Y. H. Hu, L. Wang, L. Zhang, Q. L. Zhou and N. Y. Gao, Pre-oxidation with KMnO4 changes extra-cellular organic matter's secretion characteristics to improve algal removal by coagulation with a low dosage of polyaluminium chloride, *Journal of Environmental Sciences*, 2013, **25**, 452-459.
70. F. L. Dong, Q. F. Lin, J. Deng, T. Q. Zhang, C. Li and X. D. Zai, Impact of UV irradiation on Chlorella sp. damage and disinfection byproducts formation during subsequent chlorination of algal organic matter, *Science of the Total Environment*, 2019, **671**, 519-527.
71. L. A. Coral, A. Zamyadi, B. Barbeau, F. J. Bassetti, F. R. Lapolli and M. Prévost, Oxidation of Microcystis aeruginosa and Anabaena flos-aquae by ozone: Impacts on cell integrity and chlorination by-product formation, *Water Research*, 2013, **47**, 2983-2994.
72. C. A. Mash, B. A. Winston, D. A. Meints Ii, A. D. Pifer, J. T. Scott, W. Zhang and J. L. Fairey, Assessing trichloromethane formation and control in algal-stimulated waters amended with nitrogen and phosphorus, *Environmental Science: Processes & Impacts*, 2014, **16**, 1290-1299.
73. S. Chen, J. Deng, L. Li and N. Gao, Evaluation of disinfection by-product formation during chlor(am)ination from algal organic matter after UV irradiation, *Environmental Science and Pollution Research*, 2018, **25**, 5994-6002.
74. M. Zhu, N. Gao, W. Chu, S. Zhou, Z. Zhang, Y. Xu and Q. Dai, Impact of pre-ozonation on disinfection by-product formation and speciation from chlor(am)ination of algal organic matter of Microcystis aeruginosa, *Ecotoxicology and Environmental Safety*, 2015, **120**, 256-262.

75. W. Wang, J. Sha, Z. Lu, S. Shao, P. Sun, Q. Hu and X. Zhang, Implementation of UV-based advanced oxidation processes in algal medium recycling, *Science of The Total Environment*, 2018, **634**, 243-250.
76. A. D. Pifer and J. L. Fairey, Suitability of Organic Matter Surrogates to Predict Trihalomethane Formation in Drinking Water Sources, *Environmental Engineering Science*, 2014, **31**, 117-126.
77. R. Hao, H. Ren, J. Li, Z. Ma, H. Wan, X. Zheng and S. Cheng, Use of three-dimensional excitation and emission matrix fluorescence spectroscopy for predicting the disinfection by-product formation potential of reclaimed water, *Water Research*, 2012, **46**, 5765-5776.
78. J. Xu, Z. T. Kralles, C. H. Hart and N. Dai, Effects of Sunlight on the Formation Potential of Dichloroacetonitrile and Bromochloroacetonitrile from Wastewater Effluents, *Environmental science & technology*, 2020, DOI: 10.1021/acs.est.9b06526.
79. S. Wang, T. Lin, W. Chen and H. Chen, Optimization of the precursor removal of dichloroacetonitrile (DCAN), an emerging nitrogenous disinfection by-product, in an up-flow BAC filter, *Chemosphere*, 2017, **189**, 309-318.
80. W. Qian-Yuan, L. Chao, D. Ye, W. Wen-Long, H. Huang and H. Hong-Ying, Elimination of disinfection byproduct formation potential in reclaimed water during solar light irradiation, *Water Research*, 2016, **95**, 260-267.

Table 1. Water quality of samples from Lake A, B, and C.

Sample ID	Sample Date	DOC (mg C/L)	TN (mg N/L)	NH_3-N (mg N/L)	NO_2-N (mg N/L)	NO_3-N (mg N/L)	DON[a] (mg N/L)	Br^- (mg/L)	Total Chlorophyll (μg/L)	SUVA (L mg^{-1} m^{-1})
A1	07/17/2018	4.35	7.98	0.13	0.10	8.04	NA[a]	0.01	31.77	2.71
A2	07/24/2018	4.75	7.75	0.15	0.24	7.66	NA[a]	0.02	70.37	2.65
A3	07/31/2018	7.06	6.69	0.10	0.17	6.88	NA[a]	0.02	61.53	2.28
A4	08/07/2018	4.60	6.13	0.25	0.21	5.97	NA[a]	0.01	12.23	2.57
A5	08/14/2018	4.49	5.64	0.23	0.18	5.50	NA[a]	0.02	4.70	2.36
A7	08/28/2018	3.98	4.23	0.11	0.06	4.52	NA[a]	0.02	5.00	3.76
A9	08/29/2018	5.26	5.09	0.21	0.03	4.03	0.82	0.03	32.60	2.94
A11	09/15/2018	4.46	4.68	0.20	< 0.01	4.02	0.46	0.04	70.50	3.00
A13	10/13/2018	3.72	4.81	0.16	0.01	4.07	0.57	0.04	17.30	2.81
B1	07/18/2018	3.43	2.56	0.21	0.05	1.63	0.67	0.03	34.90	2.61
B2	07/25/2018	3.77	1.43	0.13	0.06	1.19	0.05	0.02	36.00	2.44
B3	08/01/2018	4.57	0.83	0.06	0.04	0.73	0.01	0.03	36.53	1.84
B4	08/08/2018	4.82	1.34	0.18	0.07	0.50	0.59	0.02	51.60	2.34
B5	08/15/2018	7.13	0.20	0.02	< 0.01	0.02	0.16	0.05	21.53	2.04
B7	08/29/2018	4.26	1.49	0.42	0.06	0.74	0.27	0.03	20.80	1.98
B11	09/15/2018	11.98	5.79	1.16	< 0.01	0.11	4.52	< 0.01	15.70	5.40
B13	10/13/2018	5.27	6.26	0.23	0.05	5.30	0.68	0.06	25.90	1.85
C1	07/17/2018	6.89	0.39	0.03	< 0.01	0.06	0.29	0.01	45.70	1.89
C2	07/24/2018	7.82	0.52	0.03	< 0.01	0.02	0.46	< 0.01	50.03	2.01
C3	07/31/2018	6.48	0.25	0.03	< 0.01	0.04	0.17	0.01	32.37	2.00
C4	08/07/2018	6.23	0.35	0.02	< 0.01	0.01	0.31	< 0.01	40.37	1.89
C5	08/14/2018	7.68	0.46	0.02	< 0.01	0.01	0.42	< 0.01	63.10	1.84
C7	08/28/2018	7.32	0.64	0.46	< 0.01	0.04	0.14	0.01	49.40	1.81
C9	08/29/2018	9.34	1.25	0.14	< 0.01	0.04	1.08	0.02	68.40	1.77
C11	09/15/2018	6.87	1.28	0.70	< 0.01	0.14	0.44	0.04	41.40	1.81
C13	10/13/2018	8.25	1.52	0.56	< 0.01	0.33	0.63	0.04	2.60	1.25
	Min	3.43	0.20	0.02	< 0.01	0.01	NA	< 0.01	2.60	1.25
	Max	11.98	7.98	1.16	0.24	8.04	4.52	0.06	70.50	5.40

[a]NA: Not Available – Negative value was calculated after subtracting NH_3-N, NO_3-N, and NO_2-N from TN.

Table 2. Pearson's r and Spearman's ρ correlation coefficients between water quality parameters and DBP yields. A strong correlation is considered to be r, $\rho \geq |0.5|$ with $p \leq 0.05$. Statistically significant correlations are in bold text.

	THMs		HANs		TCNM		HKs	
	r	ρ	r	ρ	r	ρ	r	ρ
Total Chlorophyll	-0.2113	-0.232	-0.063	0.054	-0.163	-0.165	-0.234	-0.33
	p = 0.302	p = 0.254	p = 0.760	p = 0.792	p = 0.426	p = 0.420	p = 0.251	p = 0.100
Total Chlorophyll[a]	-0.076	0.303	-0.061	0.238	-0.142	-0,516	-0.196	-0.085
	p =0.711	p = 0.132	p =0.765	p = 0.241	p = 0.487	p = 0.446	p =0.338	p =0.679
SUVA	**0.671**	**0.739**	0.163	0.225	**0.451**	**0.662**	**0.797**	**0.337**
	p < 0.001	**p < 0.001**	p = 0.425	p = 0.27	**p = 0.021**	**p < 0.001**	**p < 0.001**	**p = 0.092**
NO_2-N	-0.038	0.245	-0.182	-0.327	**0.532**	**0.634**	**-0.553**	-0.245
	p = 0.853	p = 0.227	p = 0.373	p = 0.103	**p = 0.005**	**p = 0.001**	**p = 0.040**	p = 0.227
NO_3-N	0.083	0.358	0.116	-0.047	**0.799**	**0.863**	-0.278	0.064
	p = 0.687	p = 0.073	p = 0.572	p = 0.82	**p < 0.001**	**p < 0.001**	p = 0.169	p = 0.756
DON	0.379	0.22	0.323	**0.723**	0.096	0.398	**0.85**	**0.567**
	p = 0.099	p = 0.352	p = 0.165	**p < 0.001**	p = 0.689	p = 0.082	**p < 0.001**	**p = 0.009**
NH_3-N	0.121	0.079	0.196	0.177	-0.059	**0.39**	**0.669**	**0.487**
	p = 0.557	p = 0.701	p = 0.336	p = 0.386	p = 0.773	**p = 0.049**	**p < 0.001**	**p = 0.012**
DOC[a]	**0.726**	**0.597**	**0.480**	**0.428**	-0.337	**-0.485**	**0.610**	0.238
	p < 0.001	**p = 0.001**	**p = 0.013**	**p = 0.029**	p = 0.093	**p = 0.012**	**p = 0.001**	p = 0.242

[a]Statistical correlations were performed using the non-normalized DBP concentration.

Table 3. Water quality of samples from Lake D and PAA pre-oxidation experiments.

Sample ID	Dosing Conditions[a]	Total Chlorophyll (μg/L)	DOC (mg C/L)	ΔDOC[b] (mg C/L)	TN (mg N/L)	DON[c] (mg N/L)	NH_3-N (mg N/L)	NO_2-N (mg N/L)	NO_3-N (mg N/L)	Br- (mg/L)	pH	SUVA[d] (L mg^{-1} m^{-1})
D1	Control	4.44	6.59		1.10	0.99	0.06	< 0.01	0.05	0.10	7.91	1.68
	Low	4.44	9.23	0.88	1.10	0.99	0.06	< 0.01	0.05	0.10	NA[e]	1.69
	High	4.44	14.39	2.53	NA[e]	NA[e]	0.06	< 0.01	0.05	0.10	NA[e]	1.31
D2	Control	4.09	7.00		0.67	0.52	0.07	0.04	0.04	0.10	8.69	1.71
	Low	4.09	9.03	0.27	1.10	0.94	0.07	0.04	0.04	0.10	NA[e]	1.71
	Med	4.09	13.56	1.29	NA[e]	NA[e]	0.07	0.04	0.04	0.10	NA[e]	1.50
	High	4.09	14.57	2.30	NA[e]	NA[e]	0.07	0.04	0.04	0.10	NA[e]	1.27
D3	Control	3.40	5.59		0.69	0.54	0.07	0.03	0.05	0.11	9.91	2.02
	Low	3.40	7.97	0.62	0.74	0.60	0.07	0.03	0.05	0.11	9.55	1.62
	Med	3.40	11.93	1.07	0.74	0.58	0.07	0.03	0.05	0.11	9.64	1.58
	High	3.40	12.89	2.03	0.80	0.65	0.07	0.03	0.05	0.11	9.23	1.50
D4	Control	2.62	4.80		1.50	0.52	0.90	0.04	0.05	0.11	9.67	2.26
	Low	2.62	7.49	0.93	1.56	0.53	0.90	0.04	0.05	0.11	9.80	2.11
	Med	2.62	10.08	0.01	1.47	0.49	0.90	0.04	0.05	0.11	9.87	2.35
	High	2.62	10.78	0.71	1.54	0.55	0.90	0.04	0.05	0.11	9.58	1.95
D5	Control	3.65	5.71		0.73	0.62	0.07	< 0.01	0.04	0.09	9.91	1.71
	Low	3.65	13.85	6.38	1.10	0.99	0.07	< 0.01	0.04	0.09	9.94	0.77
	Med	3.65	12.09	1.11	0.88	0.76	0.07	< 0.01	0.04	0.09	9.85	1.42
	High	3.65	21.79	10.81	0.90	0.78	0.07	< 0.01	0.04	0.09	8.78	0.64
D6	Control	4.30	6.01		0.84	0.73	0.07	< 0.01	0.04	0.09	9.61	2.44
	Low	4.30	8.15	0.38	0.87	0.76	0.07	< 0.01	0.04	0.09	9.61	2.45
	Med	4.30	12.43	1.15	0.95	0.84	0.07	< 0.01	0.04	0.09	8.93	1.81
	High	4.30	13.75	2.47	1.01	0.90	0.07	< 0.01	0.04	0.09	7.89	1.90

[a]PAA dosing conditions: no PAA (control), initial dose of 2 mg/L with a contact time of 2 h (low), 6 mg/L with 2 h (med), and 6 mg/L with 6 h (high);
[b]ΔDOC (mg C/L) is calculated as the difference in DOC between experiment and control, after accounting for DOC increase by PAA formulation;
[c]DON is calculated as the NH_3-N, NO_2-N, and NO_3-N subtracted from the TN;
[d]SUVA was calculated using the adjusted DOC (subtracting DOC contributed by PAA and acetic acid);
[e]NA: Not available.

Figure 1. Variability in the (a) DOC, (b) DON, (c) total chlorophyll concentrations, and (d) SUVA values for Lakes A, B, and C samples. The corresponding data are shown in Table 1.

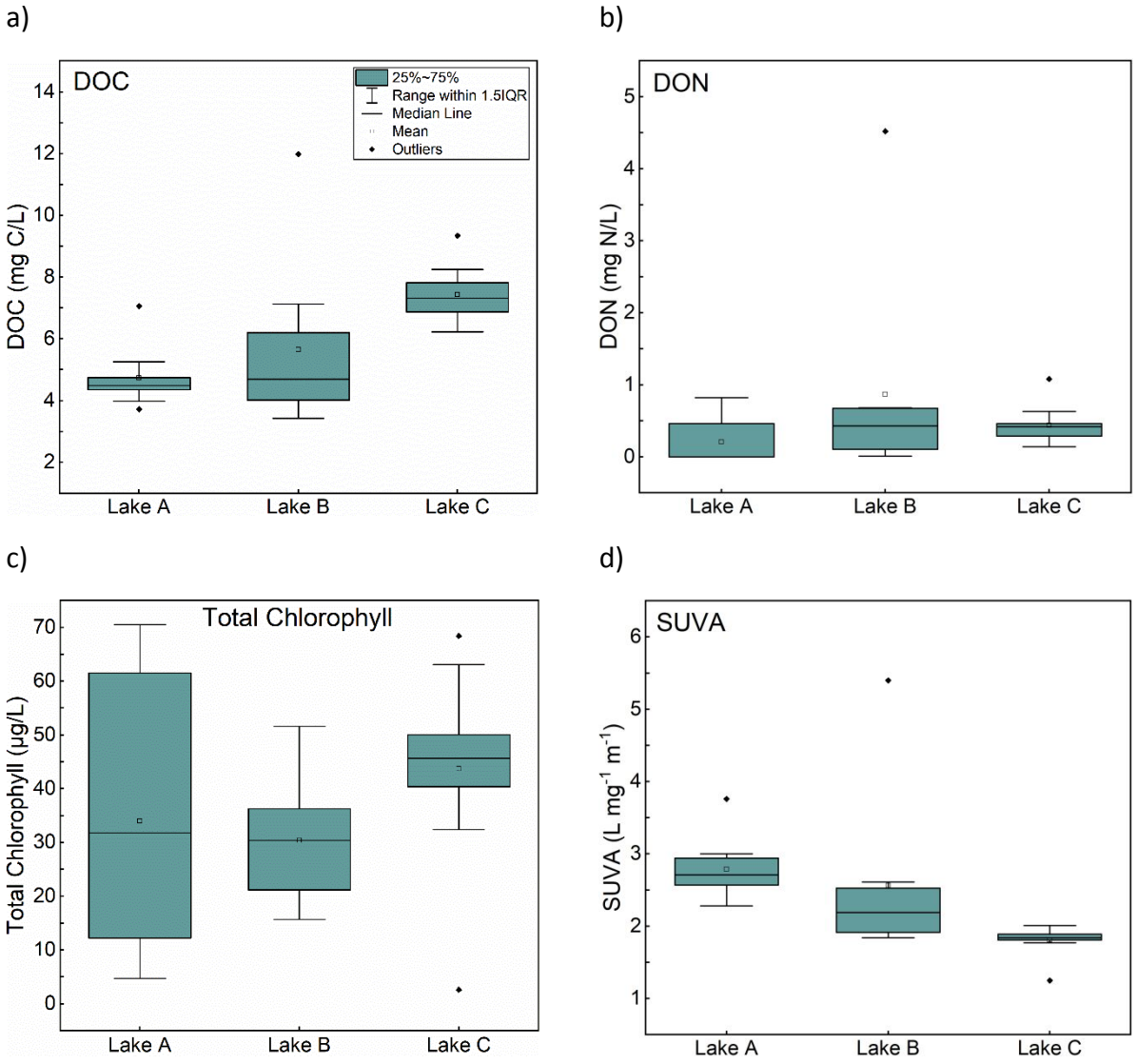

Figure 2. Variation in (a) DBP formation in UFC tests for Lake A samples and (b) the corresponding calculated cytotoxicity. HKs were not included in the calculated cytotoxicity due to unavailability of LC_{50}. Corresponding data can be found in Table S5. Similar plots for Lake B and C are shown in Figure S4.

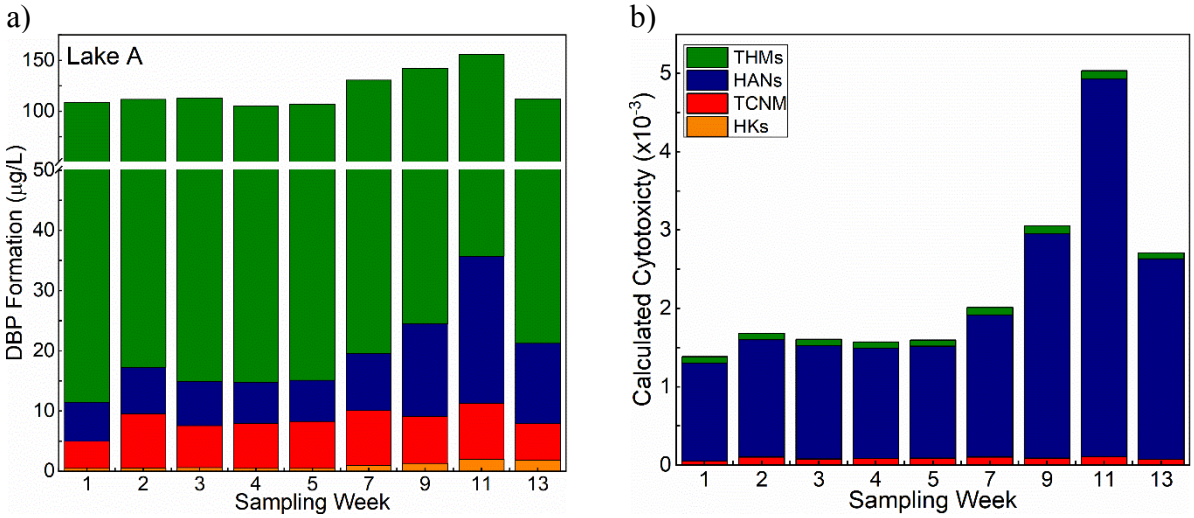

Figure 3. Temporal variation in DBP yields for samples from (a) Lake A, (b) Lake B, and (c) Lake C. The corresponding data are shown Table S5.

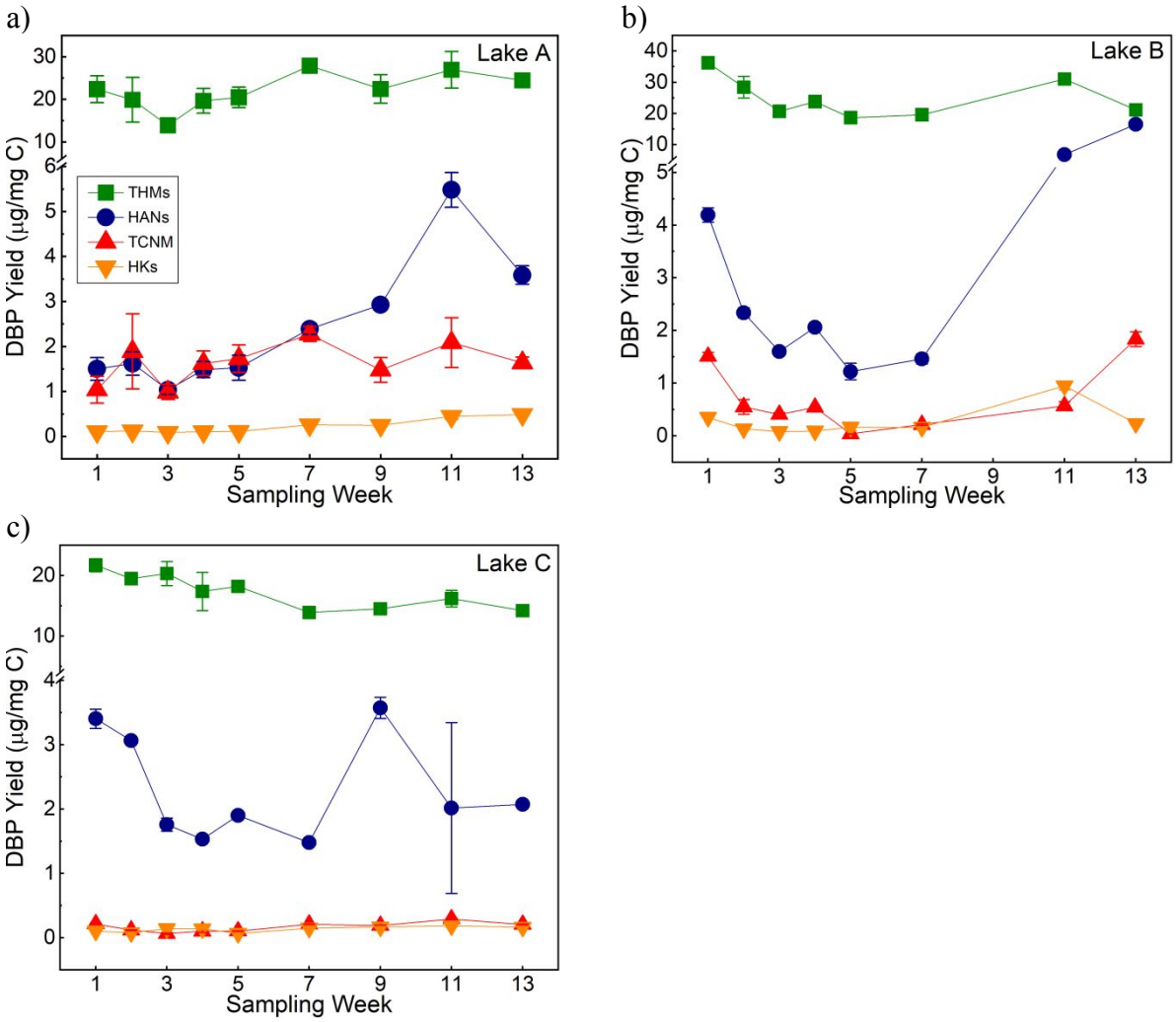

Figure 4. Relationship between total chlorophyll concentrations and the yields of (a) THMs, (b) HANs, (c) TCNM, and (d) HKs in UFC tests. Correlation statistics are reported in Table 2. Corresponding data are shown in Tables 1 and S5.

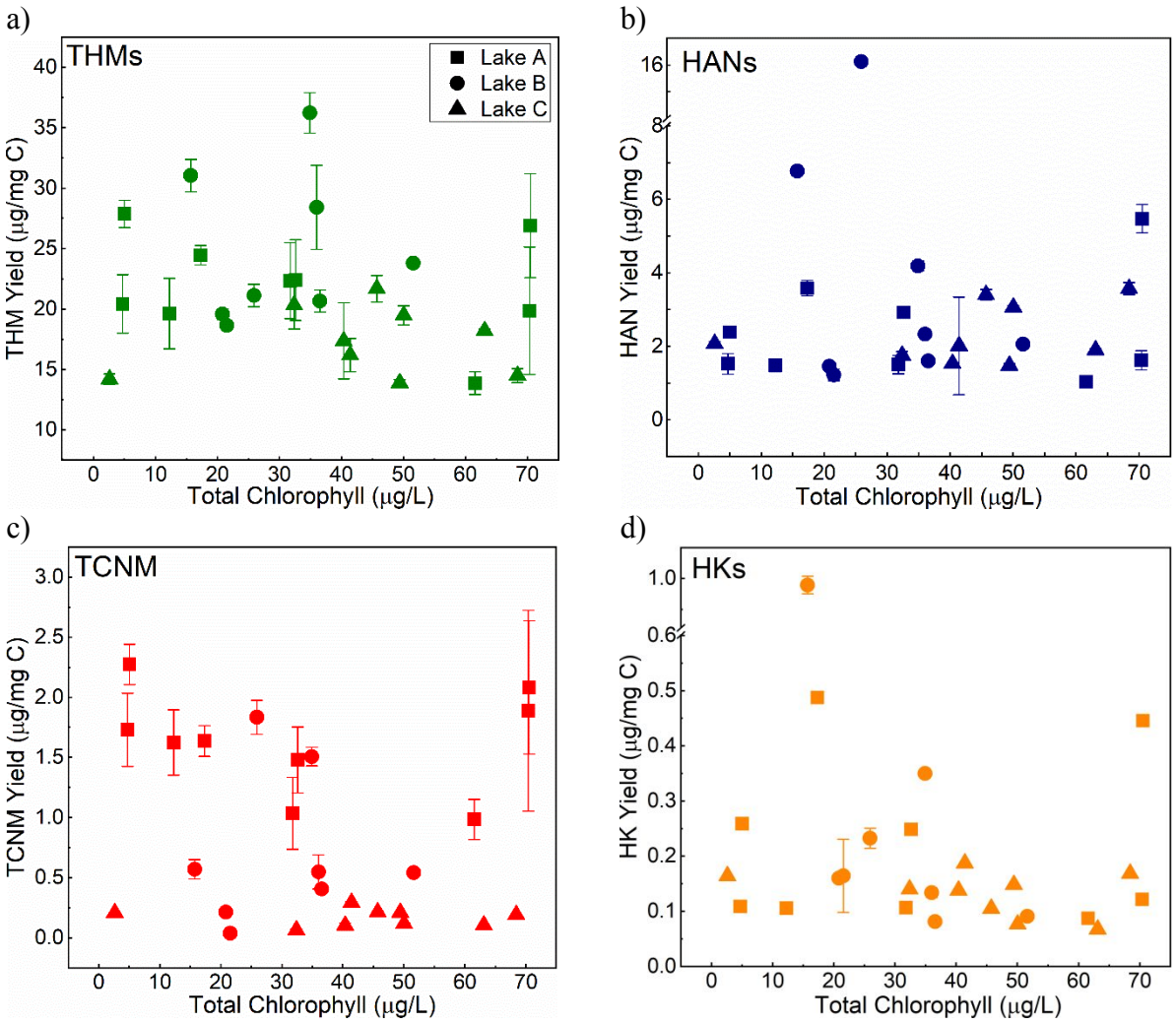

Figure 5. Change in the formation of (a) THMs, (b) HANs, (c) TCNM, and (d) HKs in the six samples from Lake D by PAA pre-oxidation. Three PAA dosing conditions were evaluated: initial dose 2 mg/L with contact time 2 h (low), 2 mg/L with 6 h (med), 6 mg/L with 6 h (high). PAA decay was considered in the calculation of exposure for each sample (section 2.5). ΔDBP Conc. = DBP concentration after UFC tests of PAA pre-oxidized samples – DBP concentration after UFC test of the corresponding control. The corresponding data are shown in Tables S4 and S7.

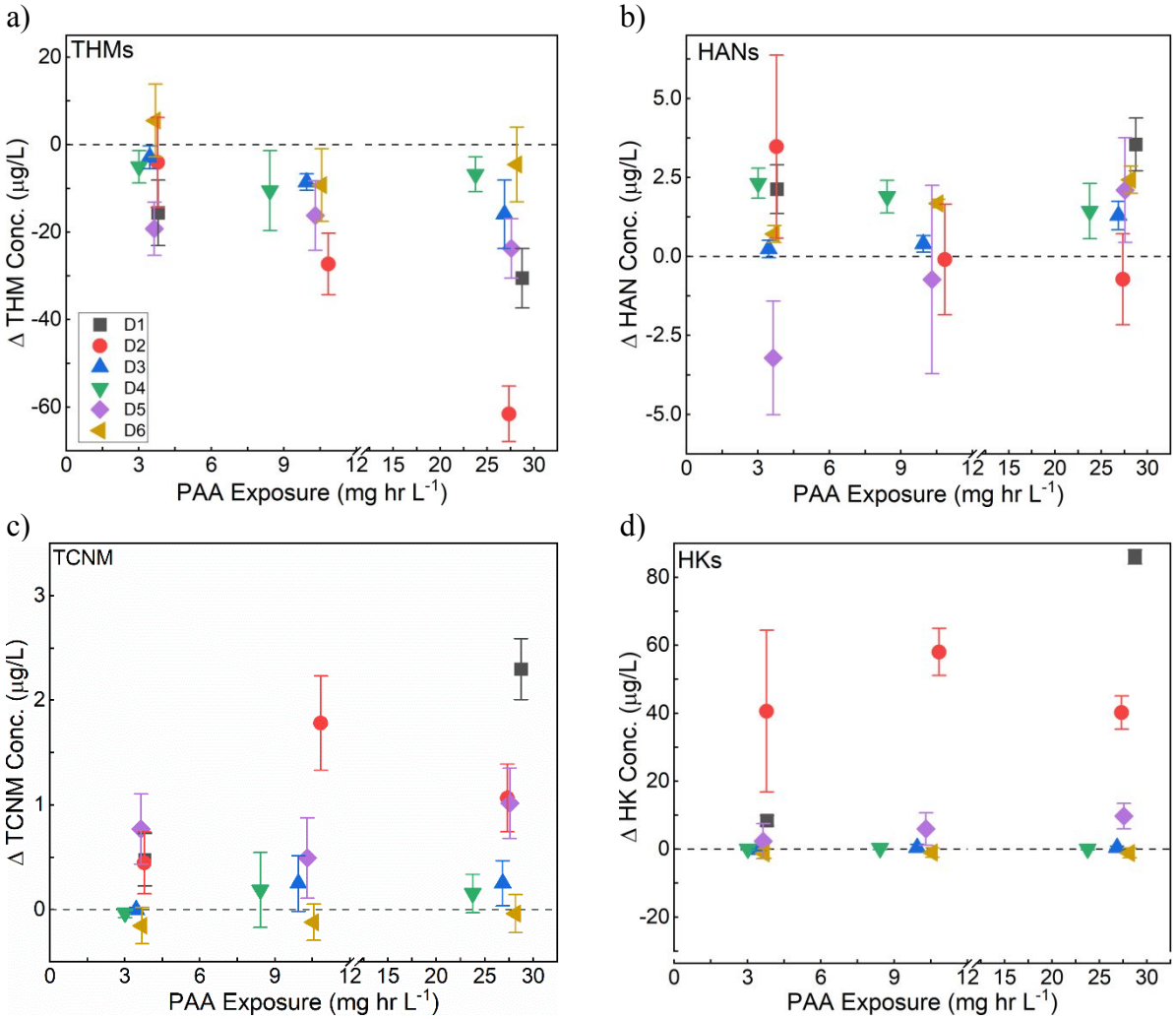

Figure 6. Percent change in the calculated cytotoxicity contributed by THMs, HANs, and TCNM by PAA pre-oxidation for six samples from different locations of Lake D. HKs are not included in the calculation of cytotoxicity. Three PAA dosing conditions were evaluated: initial dose 2 mg/L with contact time 2 h (low), 2 mg/L with 4 h (med), 6 mg/L with 6 h (high). PAA decay was considered in the calculation of exposure for each sample (section 2.5). % Change in Calculated Cytotoxicity = (calculated cytotoxicity in PAA pre-oxidized samples – calculated cytotoxicity in the corresponding control) / calculated cytotoxicity in the corresponding control. Error bars represent the propagated error. The corresponding data are shown in Table S7.

a)

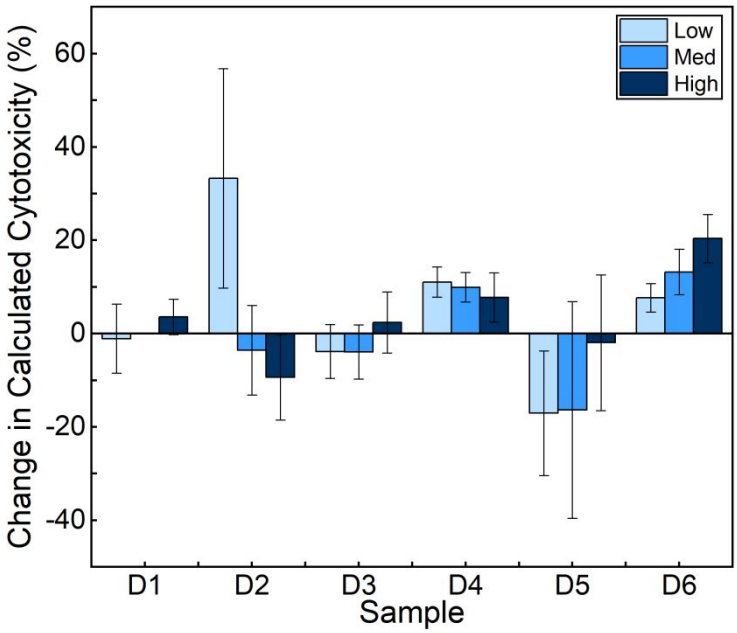

Figure 7. Change in fluorescence EEMs by PAA pre-oxidation for sample D6. Three PAA dosing conditions were evaluated: initial dose 2 mg/L with contact time 2 h (low), 2 mg/L with 6 h (med), 6 mg/L with 6 h (high).

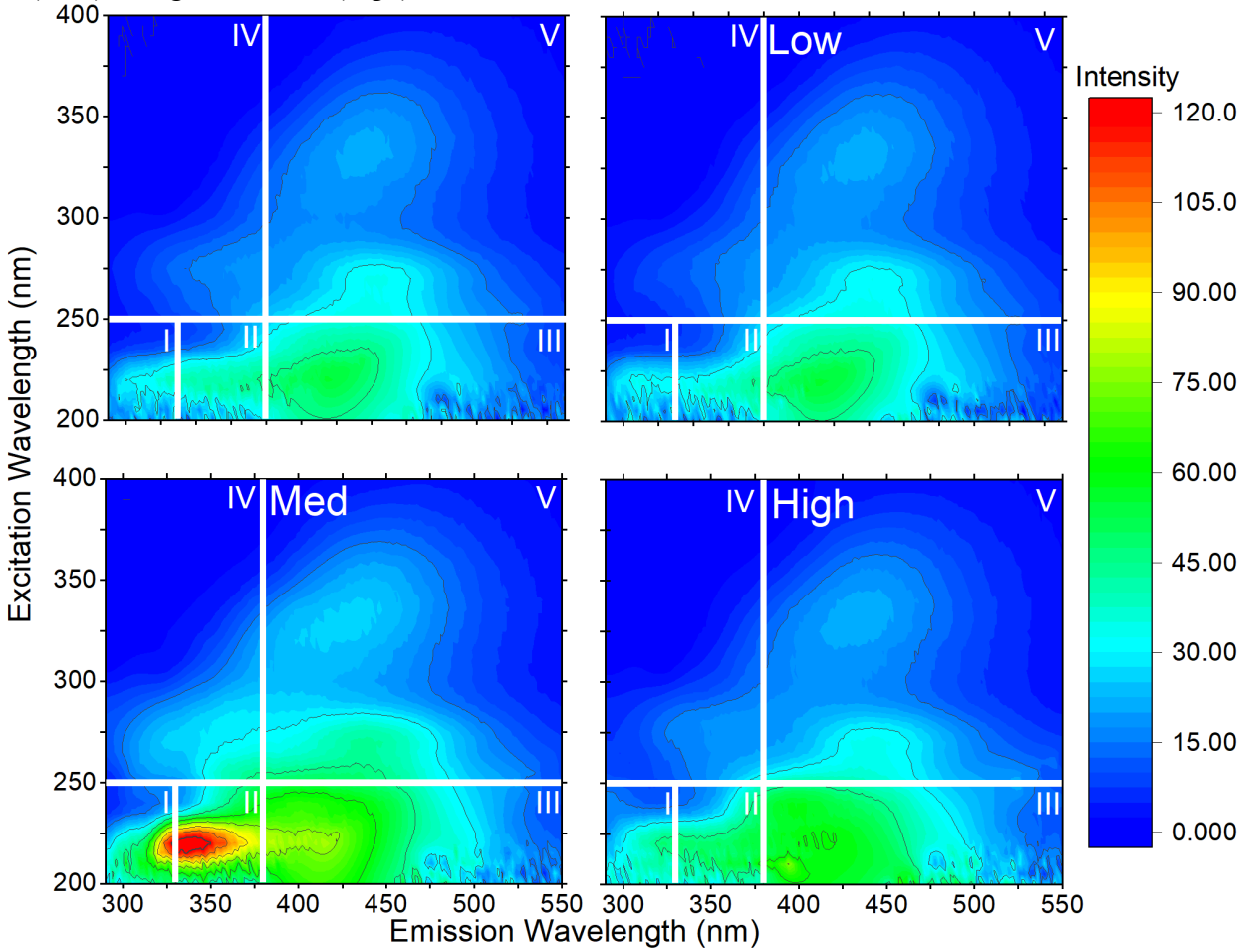

Figure 8. Change in fluoresence intensity in the (a) tyrosine-like, (b) tryptophan-like, (c) fulvic-like, (d) soluble microbial product-like, and (e) humic-like regions by PAA pre-oxidation for four samples from different locations of Lake D. PAA dosing conditions: initial dose 2 mg/L with contact time 2 h (low), 2 mg/L with 6 h (med), 6 mg/L with 6 h (high). The percent change is calculated using the corresponding control for each sample. The corresponding data can be found in Table S8.

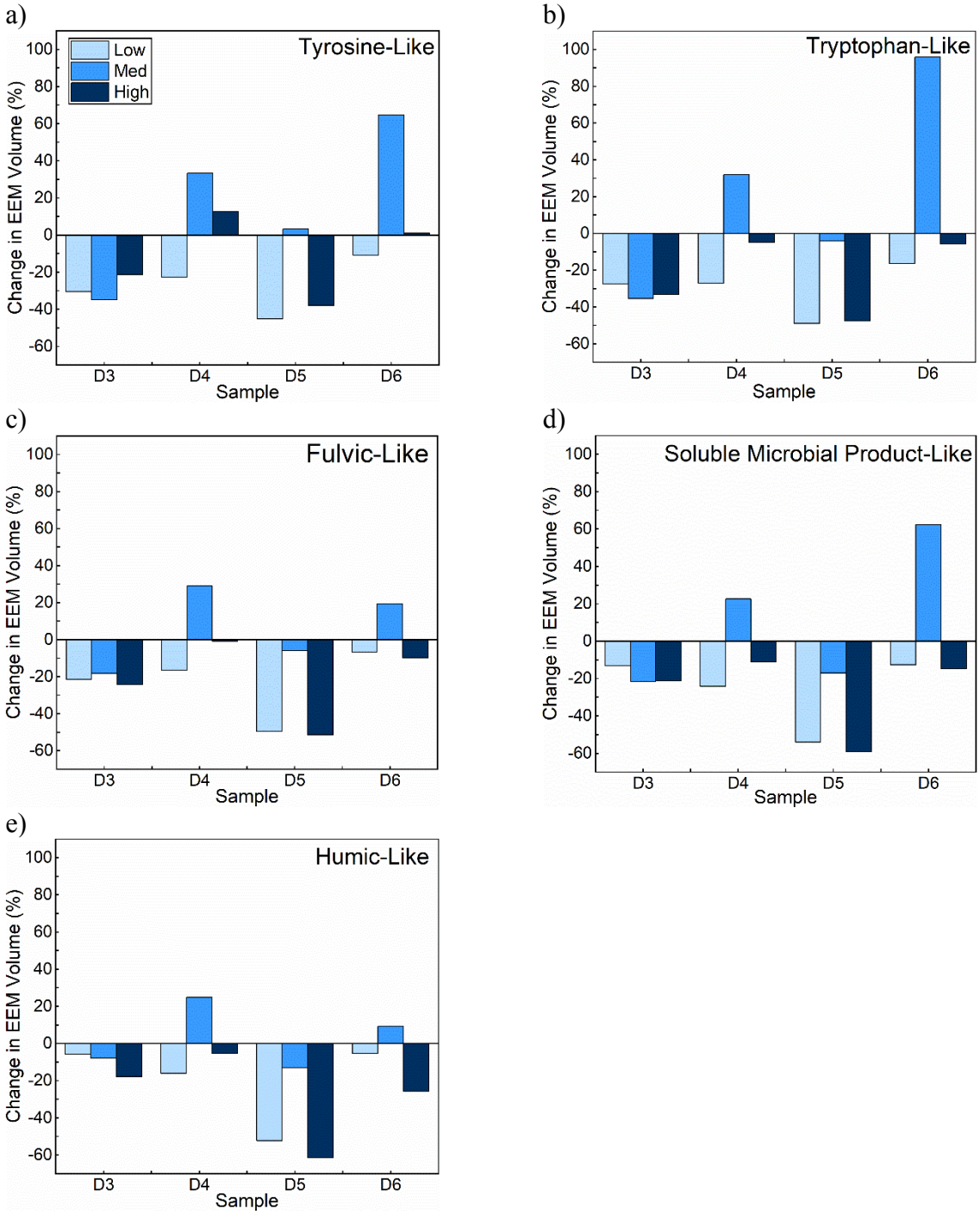

Table of Contents Entry

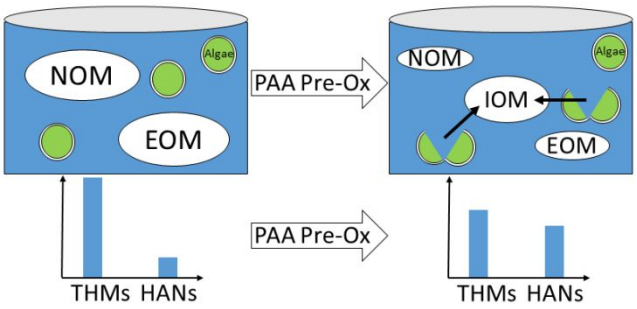

Peracetic acid pre-oxidation of algal impacted surface waters can reduce formation of trihalomethanes but promote formation of haloacetonitriles, likely due to the degradation of dissolved organic matter and coincident release of intracellular organic matter.